A New Approach for Paleostress Analysis from Kink Bands: Application of Fault-Slip Methods

Deepak C. Srivastava, Richard J. Lisle,[1] Mohd. Imran,[2] and Rajeev Kandpal

Department of Earth Sciences, University of Roorkee, Roorkee 247667, India
(*e-mail: earth@rurkiu.ernet.in*)

ABSTRACT

Optimal and nonoptimal methods of fault-slip analysis are tested on the simple type of kink bands by treating these structures as if they were striated faults. Results from different graphical and numerical techniques are mutually consistent and all imply development of these kink bands in a thrust regime as a consequence of NNW-SSE-oriented maximum compression (σ_1-axis). These results are confirmed independently by comparing the geometry of the kinks with those produced experimentally in situations in which the principal stress orientations are known. The consistency and quality of paleostress results from different methods suggest that many natural kink bands can be used to calculate paleostress in much the same way as striated brittle faults.

Introduction

Graphical and numerical techniques of fault-slip analysis are best suited to brittle faults that exhibit evidence for both direction and sense of slip (Arthaud 1969: Carey and Brunier 1974; Angelier and Mechler 1977; Etchecopar et al. 1981; Michael 1984; Lisle 1988; Angelier 1990; Hardcastle and Hills 1991; Sperner et al. 1993). These methods, however, cannot be applied in many areas where natural faults leave no evidence of sense and/or direction of slip. Furthermore, in many instances, rocks do not respond to deformation by slip on discrete surfaces. Instead, the displacement is accommodated in a tabular or lensoid zone that separates two relatively undeformed parts of the rock. Common examples of such structures include shear zones, sheared dikes, and kink bands. The significance of the former two in stress analysis has already been tested by Srivastava et al. (1995) and Lisle (1989*a*), respectively. In this article, we demonstrate that existing methods for the estimation of paleostress from striated fault data can also be used for the analysis of suitable kink band struc-

tures. We test these methods on structures bordering the Great Boundary Fault in western India.

Geological Framework of the Area

The kink bands studied are developed in the lower Cambrian sedimentary sequence juxtaposed to the Great Boundary Fault in western India (fig. 1). The Great Boundary Fault is the most conspicuous tectonic lineament in the Precambrian terrain of western India and extends for a strike length of >400 km, from Chittaurgarh in the southwest, through Satur, to Machilpur in the northeast. For much of its length, the Great Boundary Fault defines the boundary between the Archean metasediments of the Hindoli Group and the lower Cambrian sedimentary sequence of the Vindhyan Supergroup (Prasad 1984). Toward the central sector of the Great Boundary Fault near Satur, the upper Vindhyan sedimentary sequence is folded into a macroscopic, nonplunging kink fold that trends ENE-WSW (Satur anticline; Coulson 1927). The limb traces and axial trace of the Satur anticline parallel the Great Boundary Fault, and a dextral strike-slip fault offsets this anticline near Satur village (fig. 1).

In this study, we report on observations of mesoscopic kink folds developed congruently with the macroscopic kink fold (Satur anticline). These mesoscopic kink folds occur on both the limbs as well
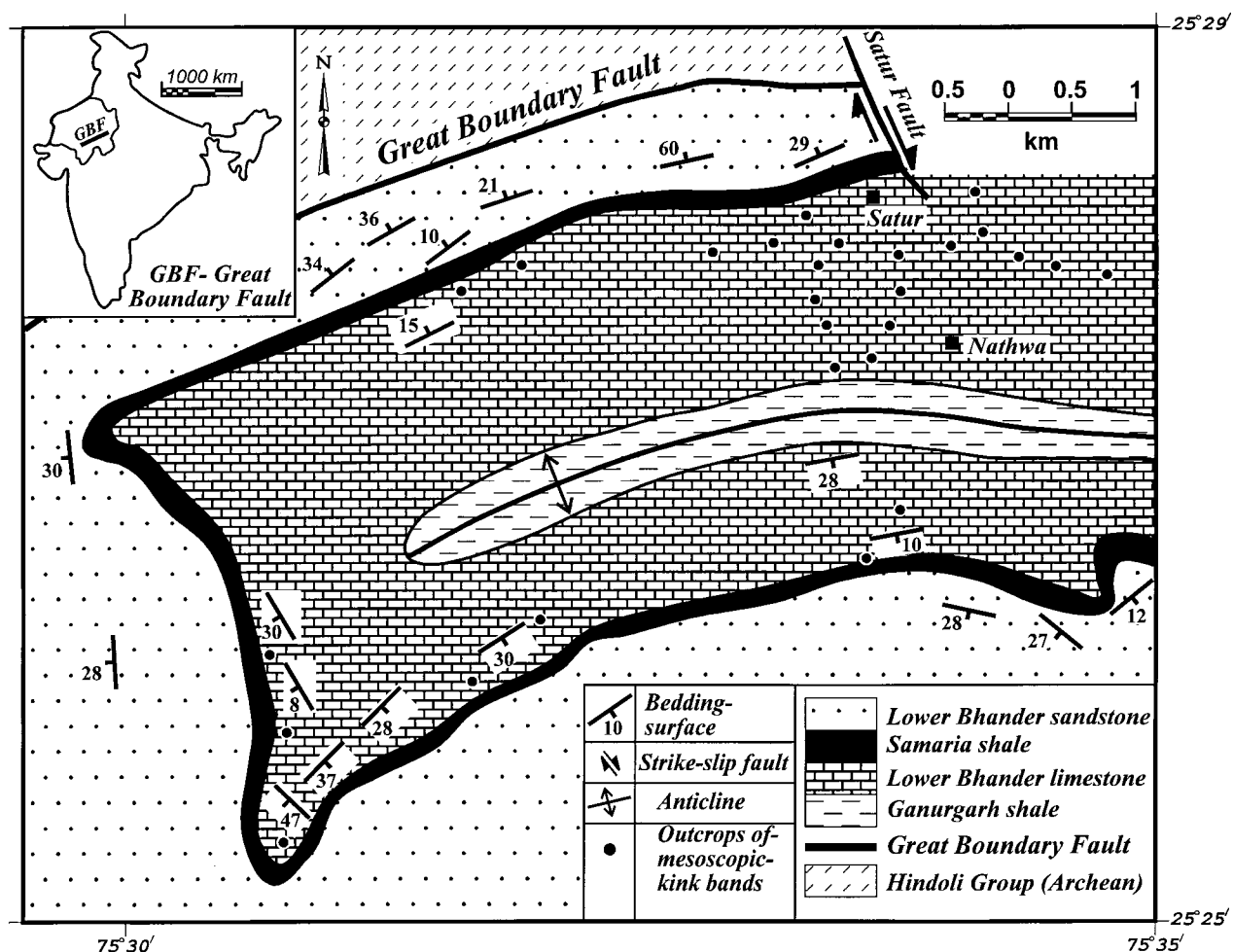
Figure 1. Geological map of the Satur Anticline (lithological contacts after Prasad 1984). Inset shows the Great Boundary Fault (*GBF*) in western India (Rajasthan).

as in the hinge zone of the Satur anticline. They are, however, best observed in the thinly bedded (centimeter scale) Lower Bhander Limestone Formation (fig. 1). Data on kink bands in the Ganurgarh Shale are not included because of poor exposures.

Geometry of the Kink Bands

Kink bands in the Satur area are mostly exposed as monoclines, but examples of conjugate pairs are also common (fig. 2). The geometry of the conjugate kinks varies from symmetric to asymmetric, and although both the fold hinge lines are essentially of a nonplunging type, their angular divergence, in map view, can range from 0° to 20°. Most of the kink bands either exhibit an orthorhombic sym-

metry or a monoclinic symmetry that approaches an orthorhombic symmetry.

External and internal foliation and kink plane are defined by the bedding surfaces and axial surface of the kink fold, respectively (fig. 3a). In most of the kink bands, the external foliation is subhorizontal to shallowly dipping, and the kink axes plunge at shallow angles (<20°) toward ENE-WSW (fig. 3b).

The deflection of foliation across the kink bands invariably implies a thrust type of movement on the kink planes. All the kink bands can be classified into two sets that correspond to conjugate pairs and imply top-to-the-NNW and top-to-the-SSE sense of movement, respectively. The relative sense of slip on kink planes is always antithetic to the sense of slip on the internal foliation within the kink bands. Layer-parallel slip during the formation of the
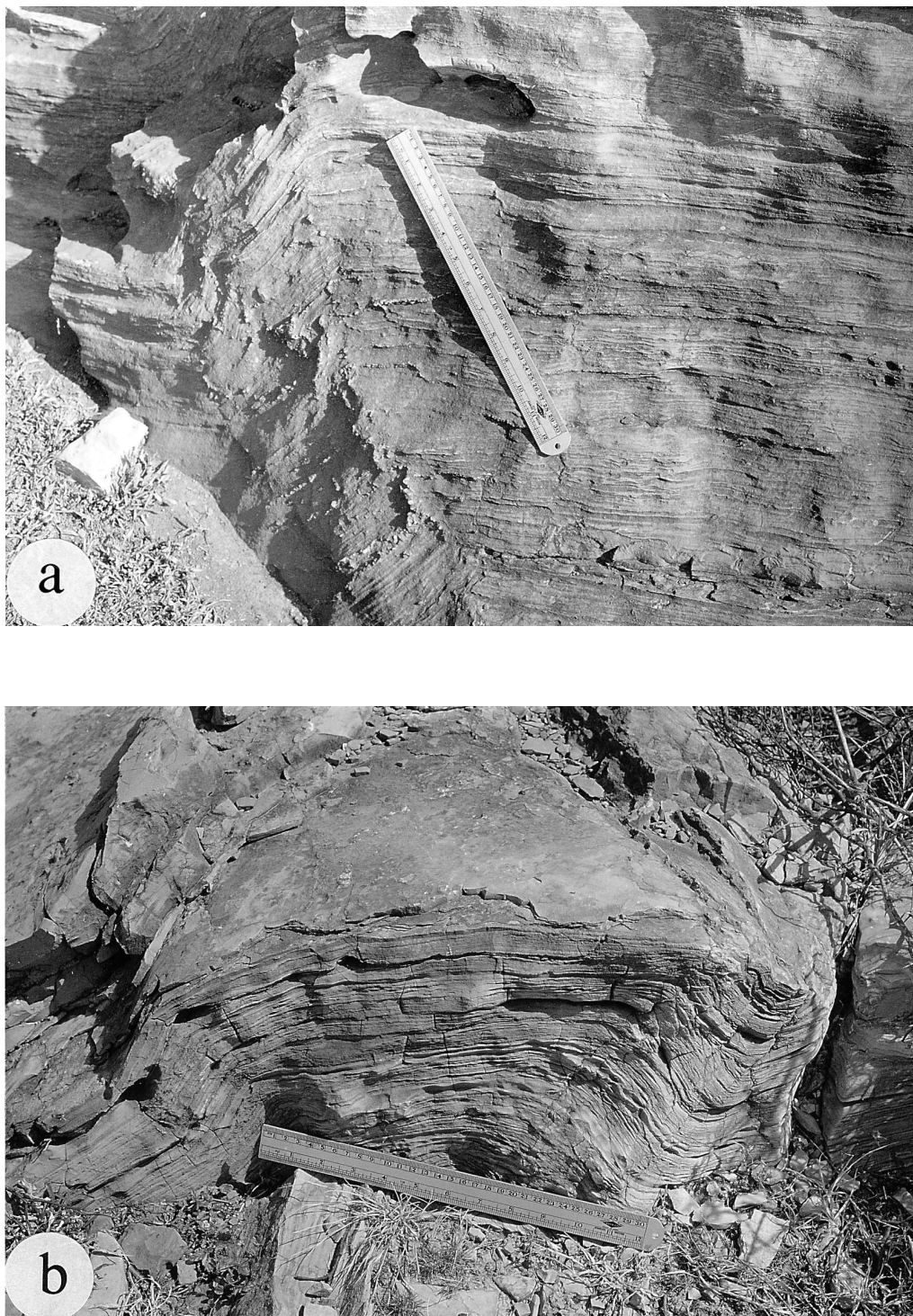
Figure 2.   Kink bands in limestone. *a*, Profile view of a top-to-the-NNW kink band exposed as a monocline (kink plane, N018° 45° E; internal foliation, N220° 75° W). *b*, A symmetric conjugate pair of kink bands. Kink planes in the kink bands on the left (top-to-the-NNW) and right (top-to-the-SSE) are oriented N100° 50° S and N090° 60° N, respectively. Kink plane in either set is parallel to the internal foliation in the complementary set.

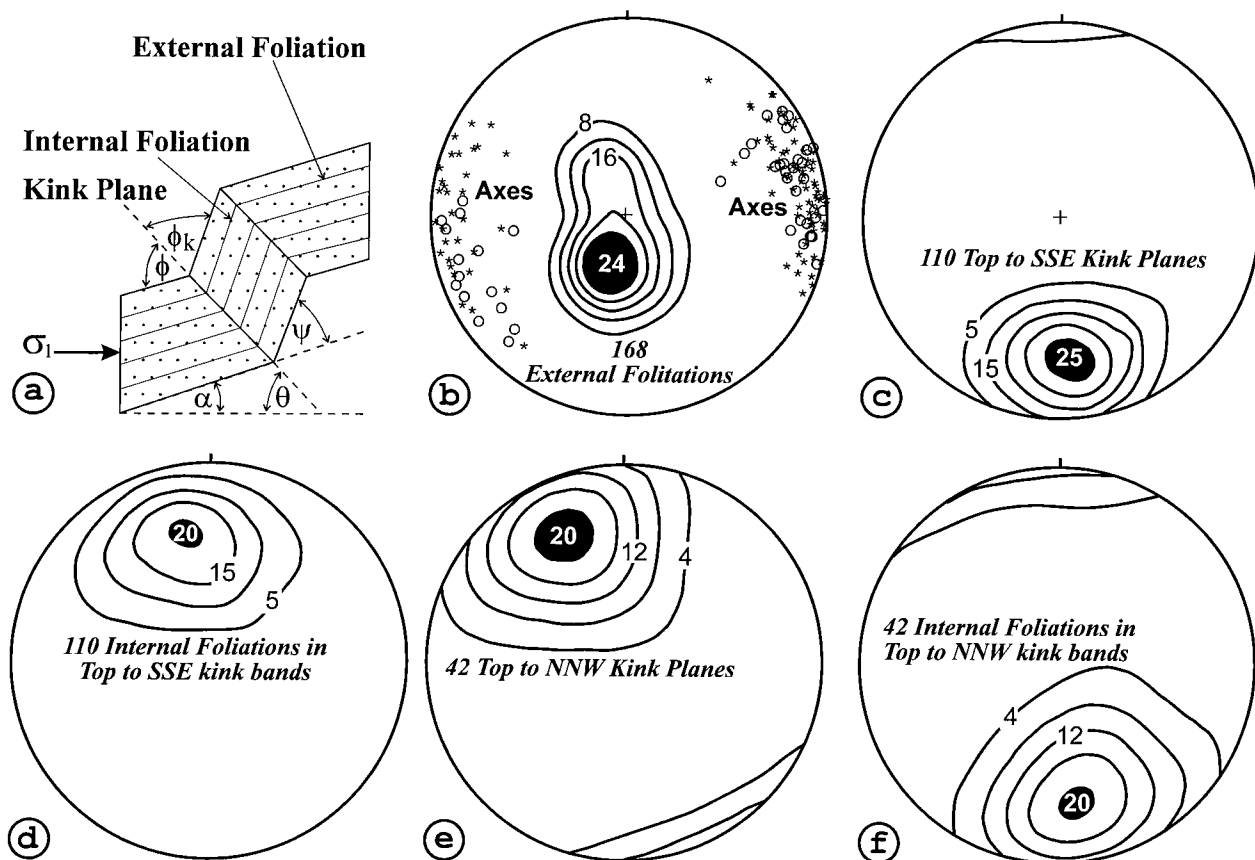**Figure 3.**   *a*, Definition of the angular parameters (ϕ, ϕ_k, and Ψ) in a kink band (after Gay and Weiss 1974). External foliation and kink plane make angles α and θ with the maximum compressive stress (σ_1-axis), respectively. *b*, Contoured poles to external foliations in kink bands. *Circles* and *stars* represent 42 axes of top-to-the-NNW and 110 axes of top-to-the-SSE kink bands, respectively. Kamb contours at every 4σ ($\sigma = 1.4$). *c–f*, Orientations of kink planes and internal foliations in the top-to-the-SSE and top-to-the-NNW sets. Kink planes in top-to-the-SSE set are parallel to the internal foliation in the top-to-the-NNW set and vice versa. Kamb contours at every 5σ ($\sigma = 1.4$) in *c* and *d* and every 4σ ($\sigma = 1.2$) in *e* and *f*.

kinks is implied by the shear offset of the preex-isting markers (e.g., vertical veins and stylolites) along the shallowly dipping bedding surfaces.

A characteristic geometrical feature of these con-jugate pairs of kink bands is the parallelism between the kink plane in one set and the internal foliation in the complementary set (figs. 2*b*, 3*c–f*). In this respect, these conjugate kink bands are geo-metrically similar to conjugate pairs of brittle-duc-tile shear zones, where the *en échelon* veins within either set are parallel to the shear zone boundary in the complementary set (type I in Beach 1975).

Paleostress Analysis

The analysis presented here is based on two as-sumptions: first, that the kink planes have the same

significance, in terms of stress, as brittle faults, and, second, that the direction of slip (resolved shear stress) on a kink plane is perpendicular to the line of intersection of the kink plane and the internal foliation within the kink band.

In support of the first assumption, it is well known that shear fractures developed in outcrops and deformation experiments pass into kink bands (e.g., Marshall 1964, fig. 1; Anderson 1974, fig. 4). Experimental simulations further suggest that whether a foliated rock responds to stress by shear fracturing (faulting) or kinking depends on (1) the material properties of the rock and (2) the selection of failure criteria (Anderson 1974); otherwise, the two modes of deformation are essentially similar. Two major differences between these two modes of deformation are that kink bands develop at higher
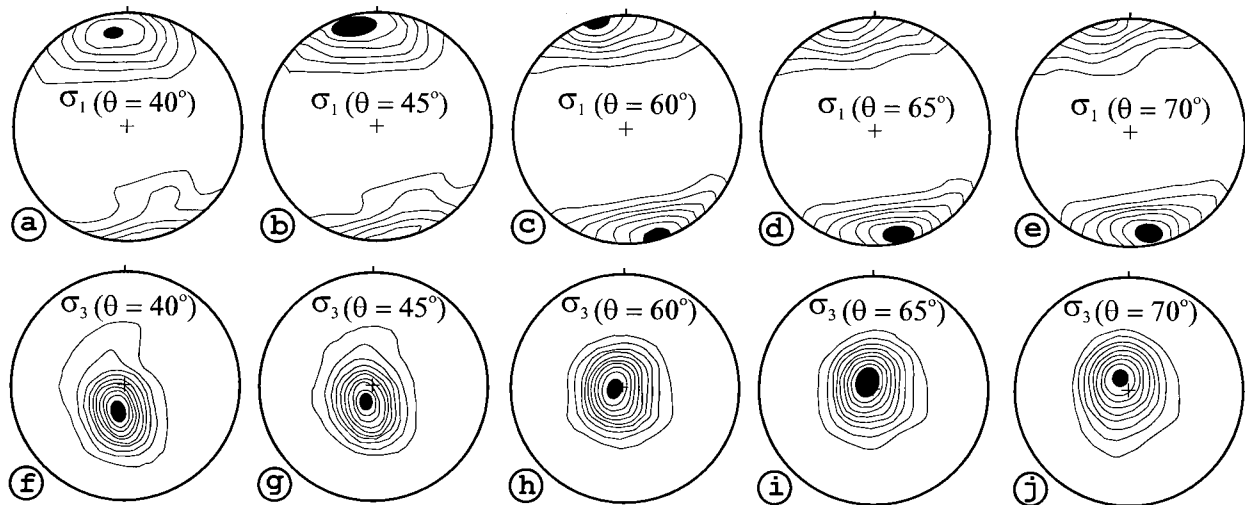
Optimal Method (P/T axis)

Figure 4.   Results from the *PT*-axis method. Same data on 152 kink bands are analyzed to obtain the orientations of σ_1- and σ_3-axes, at θ values of 40°, 45°, 60°, 65°, and 70°. Kamb contours at every 3σ ($\sigma = 1.4$) in all the diagrams.

confining pressures and are inclined at a much larger angle to the maximum compressive stress (σ_1-axis) than are shear fractures or brittle faults (Anderson 1974). Another major difference is the condition that a preexisting or intrinsic anisotropy (bedding plane or foliation) must be present for kink bands to develop. Development of brittle faults is independent of the presence of intrinsic anisotropy in the rocks. Indeed, some methods of calculating stresses from faults assume that the faulted volume of rock is mechanically isotropic.

Paleostress analyses that take intrinsic anisotropy into account include those on calcite twins (Turner 1953; Groshong 1974; Dietrich and Song 1984; and others). In these analyses, the twin plane and twin glide direction are treated dynamically similar to fault plane and slickenside lineation, respectively (Larroque and Laurent 1988). Several types of optimal and nonoptimal methods of fault-slip analysis have already been tested successfully on calcite twins (Lacombe et al. 1990; Tourneret and Laurent 1990; Shelley 1992). We extend the scope of these microscopic scale stress analyses to mesoscopic kink bands by assuming that slip direction on each kink plane makes a 90° angle from the line of intersection of the kink plane and internal foliation. In our study, this assumption is justified by the down-dip plunge of striations observable on a few kink planes and/or internal foliations. We, however, do not imply that the slip direction on all types of kink bands is perpendicular

to the line of intersection between the kink plane and internal foliation.

Methods

Paleostress methods allow the determination of different components of a geological stress tensor representing the assumed condition of homogeneous stress on the scale of analysis. Such methods fall into two classes.

Optimal Methods.   These methods assume that the slip plane and slip vector have a special orientation with respect to the stress tensor. For example, if the level of shear stress is the factor controlling whether or not slip occurs, then the most likely orientation of the principal stresses is at an angle of 45° to the slip plane. This approach implies that the observed structure is always in an optimal orientation with respect to the principal stress axes and gives rise to simple methods of stress inversion. We have used a method of this type, the *PT*-axis method, where *P*- and *T*-axes denote pressure and tension, or the maximum and minimum principal stress directions, respectively (Turner 1953; Angelier and Mechler 1977).

Nonoptimal Methods.   These methods assume that slip can occur on a variety of possible orientations relative to the principal stresses. Some methods assume that every plane is one of potential movement, though on any plane, the slip direction is governed by the direction of resolved shear stress

Table 1. Statistical Analysis of Distributions of the Orientations of Maximum (σ_1-Axis) and Minimum (σ_3-Axis) Compressive Stresses Obtained by the *PT*-Axis Method at Different Values of θ

θ	Type of distribution (K)		Strength of clustering (C)		Orthogonality test
	σ_1-axis	σ_3-axis	σ_1-axis	σ_3-axis	
40°	3.850	2.258	1.995	2.621	142.992
45°	3.926	3.700	2.164	2.672	162.443
60°	3.507	78.758	2.453	2.568	175.221
65°	4.508	15.984	2.361	2.540	170.612
70°	5.925	8.309	2.219	2.477	159.956

Note. θ = angle between kink plane and σ_1-axis; K = shape parameter; C = strength parameter; orthogonality test = degree of orthogonality between σ_1- and σ_3-axes (difference between largest and smallest eigenvalue).

on that plane. Several methods of this type have been developed during the last 2 decades (see Angelier 1994 for review). The nonoptimal methods employed in this study are the right dihedra method, right trihedra method, and direct inversion method.

Application of the Optimal Methods to the Kink Bands

The *PT*-axis method allows the individual determinations of the orientations of principal stress axes by constructing a "movement plane" (a plane perpendicular to the intersection of the kink plane and the internal foliation) for every kink band. Both σ_1- and σ_3-axes lie in the movement plane such that they are respectively inclined at angles θ and $90° + \theta$ from the slip direction (where θ is a function of the coefficient of internal friction). The knowledge of an appropriate value of θ is, therefore, an essential requirement in the application of the *PT*-axis method.

Despite the fact that some of the proposed mechanisms of kink band growth require rotation of the kink planes (Weiss 1980), the angle θ between the kink plane and σ_1-axis is found to have remained fixed in most of the natural and experimentally developed kink bands (Borg and Handin 1966; Paterson and Weiss 1966; Donath 1968; Kleist 1972). It is likely that angle θ gets locked during the early stages of kink band growth, and consequently, many natural kink planes that belong to a set, for example, those at Satur, are characterized by a consistent geometry and orientation (fig. 3c, e). Only those kink bands that can be inferred to have developed at a constant value of angle θ can be tested by the *PT*-axis method.

In general, a value of $\theta = 30°$ is recommended for the application of the *PT*-axis method on brittle faults (Ragan 1985, p. 137). This recommendation is based on two considerations: (i) the fault planes commonly make an angle θ ($45° - \varphi/2$, where φ is the angle of internal friction) with the σ_1-axis, and

(ii) the value of φ for many natural rocks can be assumed to be close to 30°. In different cases, however, kink bands are found to develop at diverse angles to the σ_1-axis: 55°–60°, in Anderson (1964); ≤45°, in Borg and Handin (1966); 58°, in Paterson and Weiss (1966) and Kleist (1972); and 47.5°, in Donath (1968). Theoretical analysis of the layer-parallel compression model supports the contention of Anderson (1964) that kink planes are inclined at an angle of ($45° + \varphi/2$) with the σ_1-axis (Collier 1978).

What is the appropriate value of θ for the application of the *PT*-axis method to kink bands? In an attempt to answer this question, we analyzed the same data on 152 kink bands with different values of θ, namely, 40°, 45°, 60°, 65°, and 70° (fig. 4). For each value of θ, all the resultant orientations of both axes (σ_1 and σ_3) were treated statistically to determine the type of distribution (K) and the strength of pattern (C) (Woodcock and Naylor 1985). The parameters K and C are defined in such a manner that $K = \ln(S_1/S_2)/\ln(S_2/S_3)$ and $C = \ln(S_1/S_3)$, where S_1, S_2, and S_3 are the largest, intermediate, and smallest eigenvalues, respectively. The orientations of σ_1- and σ_3-axes for all the considered values of θ show clustered type of distribution patterns (fig. 4). The strength of clustering (C), however, varies with the angle θ, and the strongest clusters for both the σ_1- and σ_3-axes are obtained when θ is 60° (table 1).

It is a limitation of such a statistical analysis that the data for the σ_1- and σ_3-axes are treated independently and the important condition of orthogonality between the σ_1- and σ_3-axes remains unexploited. Thus a situation may arise where the strongest clusters for σ_1- and σ_3-axes are obtained for two different values of the angle θ and/or the angle between the two strongest clusters of σ_1- and σ_3-axes is not 90°. In order to confirm that the strongest clustering of σ_1- and σ_3-axes obtained at $\theta = 60°$ is not fortuitous, the orthogonality test of Lisle (1989b) was applied to all the orientations of σ_1- and σ_3-axes for the different values of θ (40°, 45°,

60°, 65°, and 70°; fig. 4). The difference between the largest and smallest eigenvalues is found to be greatest at $\theta = 60°$ (table 1). It is, therefore, at $\theta = 60°$ that (i) the clustering is strongest and (ii) the σ_1- and σ_3-axes most closely approach being orthogonal to each other. For this reason, 60° is considered as the most appropriate value of θ for application of the PT-axis method to the kink bands at Satur. This result obtained by our independent statistical analysis matches with Collier's (1978) results of theoretical analysis.

Application of the Nonoptimal Methods to the Kink Bands

Right Dihedra and Right Trihedra Methods. The kink bands are analyzed by the right dihedra method of Angelier and Mechler (1977) and the right trihedra method of Lisle (1987). In the right dihedra method, the suitability of each three-dimensional orientation as a potential σ_1-axis is calculated and represented as a number on the stereographic output. The contours that enclose the highest and lowest values correspond respectively to the orientations of σ_1- and σ_3-axes on the stereoplots (fig. 5a). In the right trihedra method, areas containing possible orientations of σ_1- and σ_3-axes are further narrowed down by adding a movement plane (containing the pole to the kink plane and slip direction) to the right dihedron. The right trihedra analysis was carried out using the ROMSA

program of Lisle (1988), and the results are produced as separate stereoplots for the σ_1- and σ_3-axes. The contour maxima enclosing the most probable orientations of the σ_1- and σ_3-axes for all the kink bands and the total percentage of kink bands (P_{total}%) that are compatible with the solutions are shown in figure 5b, c.

Direct Inversion Method. Several numerical techniques allow the inversion of field data to determine a reduced stress tensor that comprises four components. Whereas three components of this tensor define the orientations of three principal stresses, the fourth component represents the relative magnitude of principal stresses in terms of a shape parameter, $\Phi = (\sigma_2 - \sigma_3)/(\sigma_1 - \sigma_3)$. The earlier methods were based on a grid search by assigning different values to four parameters of the reduced stress tensor until a satisfactory solution was obtained (Carey and Brunier 1974). The direct inversion method adopted here is based on solving simultaneous equations such that the average angle between the theoretically calculated direction of shear stress and the observed direction of slip is minimized and the magnitude of relative shear stress is maximized to overcome rock cohesion and friction (Angelier 1990).

An additional merit of the nonoptimal methods is that they yield the quality of solution in terms of quantitatively defined parameters, such as, ANG, RUP, COH%, and P_{total}% (Angelier 1990, 1994; Lisle 1988). The parameter ANG represents
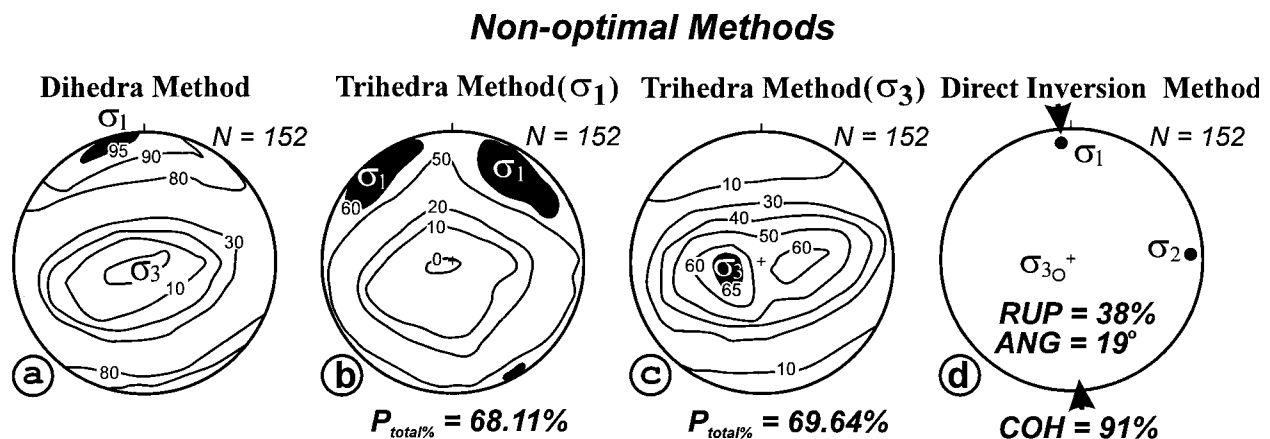
Non-optimal Methods

Figure 5. Results of paleostress analysis by fault-slip methods on the kink bands. *a*, Right dihedra method (contour maximum, 95%, and minimum, 0%, represent the orientations of the σ_1- and σ_3-axes, respectively). *b, c*, Right trihedra method (contour maxima represent orientations of σ_1-axis and σ_3-axis in *b* and *c*, respectively). P_{total}% = total% of kink bands that are compatible with the orientations of the σ_1- and σ_3-axes. *d*, Results from direct inversion method. RUP%, ANG, and COH% indicate the quality of results. ANG = the angle between observed and numerically computed directions of shear stress; RUP = a function of ANG and the level of resolved shear stress; COH% = total% of the kink bands that are satisfied with the obtained stress solution. All contours are percent per 1% area.
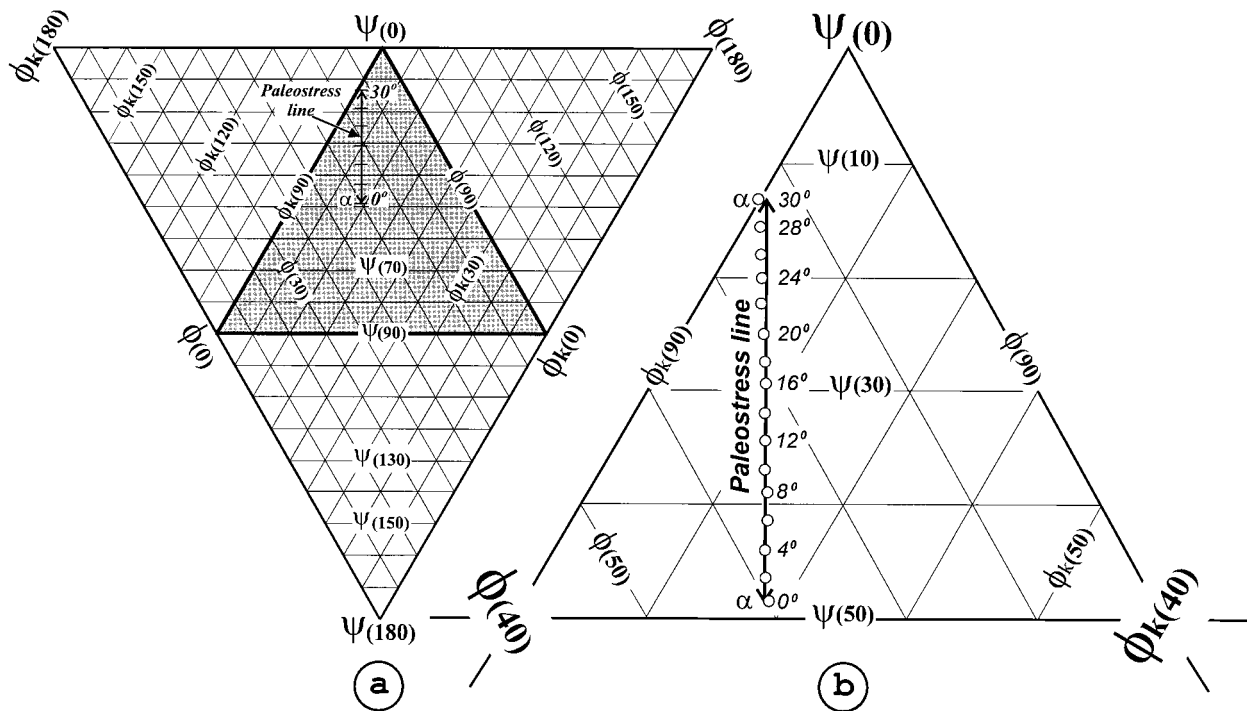
Figure 6.   *a*, Triangular graph $\phi_{(180)} - \phi_{k(180)} - \Psi_{(180)}$, for plotting the kink bands in terms of their angular parameters (ϕ, ϕ_k, and Ψ). Most natural kink bands plot within the shaded subtriangle $\phi_{(0)} - \phi_{k(0)} - \Psi_{(0)}$. *b*, Enlargement of a part of the subtriangle $\phi_{(0)} - \phi_{k(0)} - \Psi_{(0)}$ (*shaded region*, fig. 6*a*). Triangular plots of kink bands (*circles*) based on the experimental data (ϕ, ϕ_k, and Ψ angles) for different values of α between 0° and 30° (Gay and Weiss 1974). Paleostress line (*barbed*) is the best fit line ($\pm 1°$) through the plots of experimentally developed kink bands.

the average angular misfit between the direction of slip observed on the fault plane as slip lineations and the direction of shear stress computed from the reduced stress tensor. The parameter RUP is defined as the ratio of v and the magnitude of maximum shear stress computed from the reduced stress tensor; v is the modulus of vectorial difference between (i) the observed slip and (ii) the ratio of shear stress and maximum possible shear stress on a given fault plane. The parameters ANG and RUP are correlatable, and they vary between 0° and 180° and 0% and 200%, respectively. In general, results with RUP < 50% and ANG < 22.5° are considered to be good, and those with RUP between 50% and 75% and ANG between 22.5° and 45° are acceptable. Values of RUP > 75% and ANG > 45° indicate the probability of a heterogeneous data set corresponding to more than one stress tensor. The COH% implies the total number of faults that are compatible with the computed reduced stress tensor, and its significance is similar to that of P_{total}% in the right trihedra method of Lisle (1988).

Results

The orientations of the principal stress axes obtained by different types of optimal and nonoptimal methods are highly consistent (fig. 5). All the methods reveal that the kink bands were developed as a consequence of a subhorizontal maximum compression (σ_1-axis) in NNW-SSE direction and a subvertical minimum compressive stress (σ_3-axis). These orientations of principal stresses imply the origin of kink bands by layer-parallel compression in a thrust-type regime. Although the Great Boundary Fault is also known to be a thrust in the study area (Iqbaluddin et al. 1978), there is no conclusive evidence to suggest that the kinking was synkinematic with the thrusting on the Great Boundary Fault.

High values of P_{total}% (68%–70%) obtained from the right trihedra method, and COH% (91%) from the direct inversion method, suggest that most of the kink bands are compatible with the calculated stress tensors (fig. 5*b–d*). Low average values of the parameters of ANG (19°) and RUP (38%) obtained
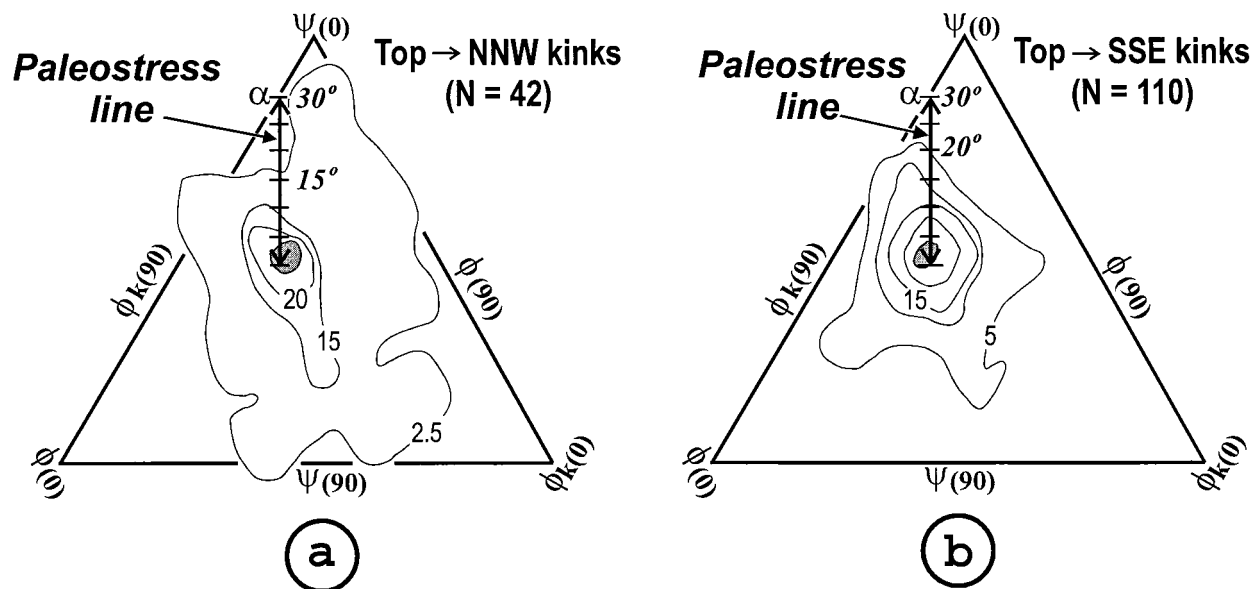
Figure 7.   *a, b,* Contours for triangular plots of the two sets of kink bands in Satur area. 25% contour maxima (shaded in gray) in both the sets lie at $\alpha = 0°$ on the paleostress line (tick marks on the paleostress line are at every 5° interval in α angle). All contours are drawn as percent per 1% of the area on the triangular graph $\phi_{(180)} - \phi_{k(180)} - \Psi_{(180)}$. After Srivastava et al. 1998; reproduced with permissions from Elsevier Science, Oxford, and authors.

from the direct inversion method (fig. 5*d*) imply that the quality of solutions is very good (Angelier 1994). Our study demonstrates that the quality of the results on kink bands is as good as the results from analysis on brittle faults and much better than the results obtained by application of fault-slip methods on the brittle ductile and ductile shear zones (Srivastava et al. 1995).

Independent Test of the Results

The geometry of a kink band is constrained by three angular parameters, namely, ϕ, ϕ_k, and Ψ (defined in fig. 3*a*). Gay and Weiss (1974) produced kink bands of different geometries in card decks and slate by varying the angle (α) between maximum compression (σ_1) and the anisotropy from 0° to 30°. Their experimental results reveal that each of the three angular parameters (ϕ, ϕ_k, and Ψ) varies linearly with the systematic change in the orientation of the σ_1-axis (measured in terms of the angle α, fig. 3*a*). Gay and Weiss (1974) were able to decipher the α angles for a large number of natural kink bands by comparing their ϕ and Ψ angles with the experimentally obtained linear relationships (ϕ vs. α and Ψ vs. α).

The angular parameters in a kink band are always related by an equation, $\phi + \phi_k + \Psi = 180°$ (fig. 3*a*). This condition can be used to construct a triangular

graph $\phi_{(180)} - \phi_{k(180)} - \Psi_{(180)}$ for representing the geometry of a kink band (fig. 6*a*). The angles ϕ, ϕ_k, and Ψ are respectively equal to 180° at the three apices of the triangular graph, and each of these angles decreases progressively down to 0° along its respective bisector of the apical angle (fig. 6*a*). The three angles (ϕ, ϕ_k, and Ψ) required to plot a kink band on the triangular graph are measurable readily on the profile sections of natural kink bands. It is observed that most natural kink bands plot within the subtriangle $\phi_{(0)} - \phi_{k(0)} - \Psi_{(0)}$ (shaded in fig. 6*a*).

For any value of the α angle between 0° and 30°, the three angular parameters (ϕ, ϕ_k, and Ψ) can be determined from the three experimentally established linear relationships between ϕ and α, ϕ_k and α, and Ψ and α (Gay and Weiss 1974, fig. 6). The angular parameters (ϕ, ϕ_k, and Ψ) corresponding to different values of α are determined from the experimental relationships and plotted as a set of points on the triangular graph (circles in fig. 6*b*). The paleostress line is a best fit line that can be drawn through these plots within an uncertainty of $\pm 1°$ (fig. 6*b*; Srivastava et al. 1998). For a natural kink band that plots on the paleostress line, the value of angle α can be read directly (fig. 6*b*). Once the ϕ and α angles are known from the angular measurements on the profile section of a kink band (fig. 3*a*) and the relative position of the kink band plot on the paleostress line (fig. 6*b*), respectively,
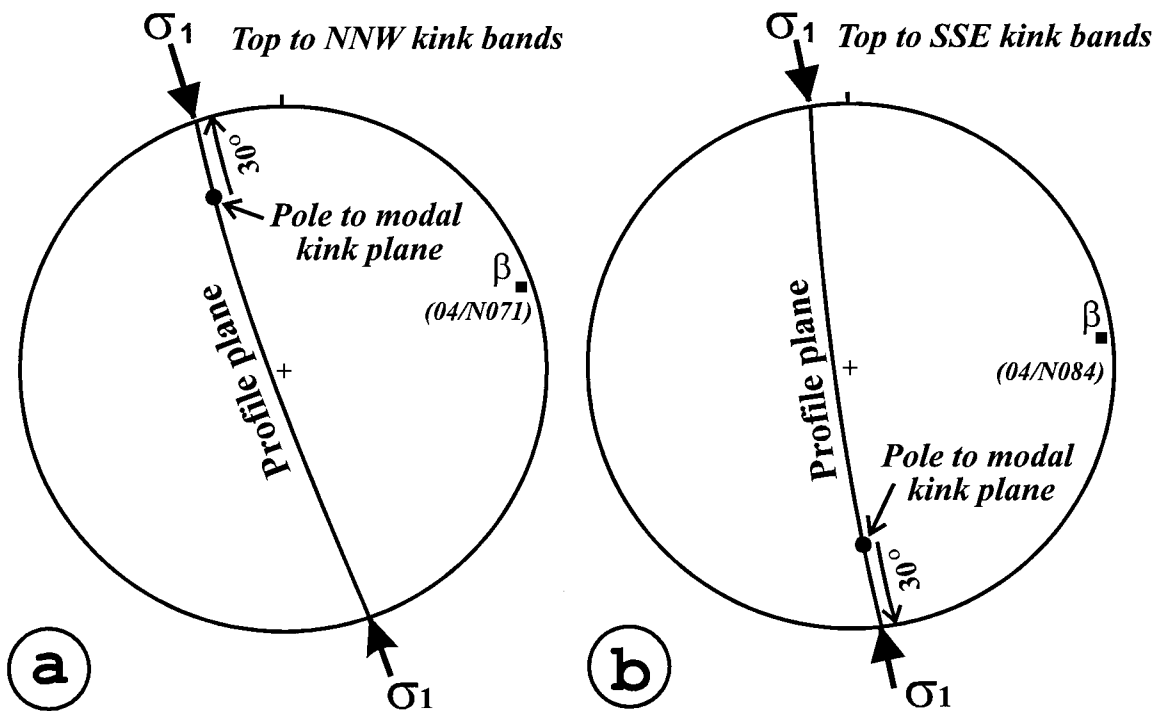
Figure 8. *a*, *b*, Stereoplots showing the orientations of σ_1-axes in top-to-the-NNW and top-to-the-SSE kink bands, respectively. As ϕ and α are equal to 60° and 0°, respectively, the θ angle ($= \phi - \alpha$) is equal to 60° for both sets. The σ_1-axis is oriented at an angle of 30° (90° $- \theta$) from the pole to the kink plane, measured in the direction of the movement of the top.

the inclination θ of the σ_1-axis with respect to the anisotropy (external foliation) can be calculated from the equation $\theta = \phi - \alpha$.

The angular parameters ϕ, ϕ_k, and Ψ are determined stereographically from the field data on 42 top-to-the-NNW and 110 top-to-the-SSE kink bands in the Satur area. With the help of these angular parameters, the kink bands in each set are plotted and contoured (percent per 1% area) on the triangular graph $\phi_{(180)} - \phi_{k(180)} - \Psi_{(180)}$. The contoured plots reveal that the 25% maxima for both sets of kink bands fall on the paleostress line at $\alpha = 0°$ (fig. 7). As most of the kink bands at Satur are characterized by $\phi = 60°$, the angle θ between σ_1-axis and kink planes must be 60° ($\theta = \phi - \alpha$). The σ_1-axis lies on the profile plane of the kink band in such a manner that it makes an angle of 30° (90° $- \theta$) from the pole to the kink plane, measured in the direction of the relative movement of the top (fig. 8). The orientations of σ_1-axes obtained by this approach indicate a horizontal compression in the NNW-SSE direction for both the sets of kink bands. These results are consistent with the orientation of the σ_1-axis obtained from graphical and numerical methods of fault-slip analysis (figs. 4, 5).

A further testimony to these results is provided by the statistical analysis in the *PT*-axis method, suggesting that the most likely angle θ between the σ_1-axis and kink planes is 60° (table 1).

Discussion

Mesoscopic conjugate kink bands have been used successfully as paleostress indicators (e.g., Ramsay 1962; Naha and Halyburton 1974; and others). The method adopted in these analyses involved the simple approach of finding the orientations of principal stress axes by bisecting the dihedral angles. Such an approach is inapplicable in those areas where the kink bands are monoclinal and conjugate sets are not present. In our example, the data come from diversely oriented kinks exposed as monoclinal as well as conjugate kink bands of dominantly orthorhombic symmetry (fig. 2). For such a mixed data set, both the graphical and numerical techniques of fault-slip analysis yield results consistent with the experimental data of Gay and Weiss (1974) and match in terms of quality the results from ideal data sets of natural striated faults. One distinct merit of kink bands over faults is that the obser-

vations on the angular relationship between the kink plane and internal foliation always imply an unambiguous sense of relative movement. The sense of relative movement can often be ambiguous on many striated brittle faults.

A prime limitation for application of the fault-slip methods to kink bands is the assumption that the direction of resolved shear stress on each kink plane is oriented at 90° to the line of intersection of kink plane and internal foliation. Another limitation of this approach is the fact that the fault-slip methods are ideally suited on reactivated surfaces of diverse orientation, whereas the kink bands develop as fresh structures. The high quality of results reported here is, at least partly, due to the orthorhombically symmetric geometry in bulk of the kink bands (contour maximum of the poles to external foliations is parallel to the σ_3-axis; figs. 3–5).

As a consequence, there is a statistical parallelism among σ_2-axis, both the fold hinge lines and the intersection line of the conjugate kink planes, and our assumption of slip direction being located at 90° from the kink axis are applicable correctly. Whereas these kink bands yield highly consistent orientations of the principal stresses by different methods, they are of little significance for determination of the relative magnitude of stress (shape parameter Φ) on account of their conjugate nature.

The fault-slip methods remain to be tested on the kink bands of lower symmetry and those where the σ_2-axis does not lie on the external foliation plane. In such cases, neither the kink axis nor the σ_2-axis will be parallel to each other, nor will the assumption of orthogonality between slip direction and kink axis hold good. Independent evidence indicating the direction of movement (shear stress) on kink planes of lower symmetry is mandatory.

Conclusions

Application of fault-slip methods to the kink bands of orthorhombic symmetry yields high-quality paleostress results. These methods can be used as an alternative to other graphical methods for paleostress analysis from kink bands. Whether or not the fault-slip methods would yield high-quality stress solutions on the kink bands of lower symmetry remains to be tested.

REFERENCES CITED

Anderson, T. B. 1964. Kink bands and related geological structures. Nature 202:272–274.

———. 1974. The relationship between kink-bands and shear fractures in the experimental deformation of slate. J. Geol. Soc. Lond. 130:367–382.

Angelier, J. 1990. Inversion of field data in fault tectonics to obtain regional stress. III. A new rapid direct inversion method by analytical means. Geophys. J. Int. 103:363–376.

———. 1994. Fault-slip analysis and paleostress reconstruction. *In* Hancock, P. L., ed. Continental deformation. Pergamon, Oxford, p. 53–100.

Angelier, J., and Mechler, P. 1977. Sur une méthode graphique de recherche des contraintes principales également utilisable en tectonique et en séismologie: la méthode des dièdres droits. Bull. Soc. Geol. Fr. 7: 1309–1318.

Arthaud, F. 1969. Méthode de détermination graphique des directions de raccourcissement, d'allongement et intermédiaire d'une population de failles. Bull. Soc. Geol. Fr. 7:729–737.

Beach, A. 1975. The geometry of *en échelon* vein arrays. Tectonophysics 28:245–263.

Borg, I., and Handin, J. 1966. Experimental deformation of crystalline rocks. Tectonophysics 3:249–368.

Carey, E., and Brunier, B. 1974. Analyse théorique et numérique d'un modèle mécanique élémentaire appliqué à l'étude d'une population de failles. C. R. Acad. Sci. Paris D279:891–894.

Collier, M. 1978. Ultimate locking angles for conjugate and monoclinal kink bands. Tectonophysics 48: T1–T6.

Coulson, A. L. 1927. The geology of Bundi state, Rajasthan. Rec. Geol. Surv. India 60:153–204.

Dietrich, D., and Song, H. 1984. Calcite fabrics in a natural shear environment: the Helvetic nappes of western Switzerland. J. Geol. 6:19–32.

Donath, F. A. 1968. Experimental study of kink-bands in Martinsburg slate. *In* Baer, A. J., and Norris, D. K.,

eds. Researches in tectonics. Geol. Surv. Can. Pap. 68-52, p. 255–288.

Etchecopar, A.; Vassuer, G.; and Daignieres, M. 1981. An inverse problem in microtectonics for determination of stress tensors from fault striation analysis. J. Struct. Geol. 3:51–65.

Gay, N. C., and Weiss, L. E. 1974. The relationship between principal stress directions and the geometry of kinks in foliated rocks. Tectonophysics 21:287–300.

Groshong, R. H., Jr. 1974. Experimental test of least square strain gauge calculation using twinned calcite. Geol. Soc. Am. Bull. 85:1855–1864.

Hardcastle, K. C., and Hills, L. S. 1991. BRUTE3 and SELECT: Quick Basic 4 programs for determination of stress tensor configurations and separation of heterogeneous populations of fault-slip data. Comput. Geosci. 17:23–43.

Iqbaluddin; Prasad, B.; Sharma, S. S.; Mathur, R. K.; Gupta, S. N.; and Sahai, T. N. 1978. Genesis of the great boundary fault of Rajasthan, India: proceedings of the third Regional Conference on Geology and Mineral Resources of Southeast Asia. Asian Institute of Technology, Bangkok, p. 145–149.

Kleist, J. R. 1972. Kink bands along Denali fault, Alaska. Geol. Soc. Am. Bull. 83:3487–3490.

Lacombe, O.; Angelier, J.; Laurent, P.; Bergerat, F.; and Tourneret, C. 1990. Joint analysis of calcite twins and fault slips as a key for deciphering polyphase tectonics: Burgundy as a case study. Tectonophysics 182: 279–300.

Larroque, J. M., and Laurent, P. 1988. Evolution of stress field pattern in the south of the Rhine graben from the Eocene to the Present. Tectonophysics 148:41–58.

Lisle, R. J. 1987. Principal stress orientations from faults: an additional constraint. Ann. Tecton. 1:155–158.

———. 1988. ROMSA: a BASIC program for paleostress analysis using fault-striation data. Comput. Geosci. 14:255–259.

———. 1989a. Paleostress analysis from sheared dike sets. Geol. Soc. Am. Bull. 101:968–972.

———. 1989b. The statistical analysis of orthogonal orientation data. J. Geol. 97:360–364.

Marshall, B. 1964. Kink bands and related geological structures. Nature 204:772–774.

Michael, A. 1984. Determination of stress from slip data: fault and folds. J. Geophys. Res. B89:11,517–11,526.

Naha, K., and Halyburton, R. V. 1974. Late stress systems deduced from conjugate folds and kink bands in the main Raialo syncline, Rajasthan, India. Geol. Soc. Am. Bull. 85:251–256.

Paterson, M. S., and Weiss, L. E. 1966. Experimental deformation and folding in phyllite. Geol. Soc. Am. Bull. 77:343–374.

Prasad, B. 1984. Geology, sedimentation and paleogeography of Vindhyan Supergroup, south-eastern Rajasthan. Geol. Surv. India Mem. 116, 107 p.

Ragan, D. M. 1985. Structural geology: an introduction to geometrical techniques. 3d ed. Wiley, New York, 393 p.

Ramsay, J. G. 1962. The geometry of conjugate kink systems. Geol. Mag. 99:516–526.

Shelley, D. 1992. Calcite twinning and determination of paleostress orientations: three methods compared. Tectonophysics 206:193–201.

Sperner, B.; Ratschbacher, L.; and Ott, R. 1993. Fault-straic analysis: a Turbo Pascal program package for graphical presentation and reduced stress tensor calculation. Comput. Geosci. 19:1361–1388.

Srivastava, D. C.; Lisle, R. J.; Imran, M.; and Kandpal, R. 1998. The kink-band triangle: a triangular plot for paleostress analysis from kink bands. J. Struct. Geol. 20: 1579–1586.

Srivastava, D. C.; Lisle, R. J.; and Vandycke, S. 1995. Shear zones as a new type of paleostress indicators. J. Struct. Geol. 17:663–676.

Tourneret, C., and Laurent, P. 1990. Paleostress orientations from calcite twins in the north Pyrenean foreland, determined by the Etchecopar inverse method. Tectonophysics 180:287–302.

Turner, F. J. 1953. Nature and dynamic interpretation of deformation lamellae in calcite of three marbles. Am. J. Sci. 251:276–298.

Weiss, L. E. 1980. Nucleation and growth of kink bands. Tectonophysics 65:1–38.

Woodcock, N. H., and Naylor, M. A. 1985. Randomness testing in three-dimensional orientation data. J. Struct. Geol. 5:539–548.